Available online at www.sciencedirect.com
SCIENCE DIRECT
Journal of Molecular Structure 786 (2006) 105–111
Journal of MOLECULAR STRUCTURE
www.elsevier.com/locate/molstruc

Electronic spectroscopy of polycyclic aromatic hydrocarbons (PAHs) at low temperature in the gas phase and in helium droplets

A. Staicu [a,b], S. Krasnokutski [a], G. Rouillé [a], Th. Henning [b], F. Huisken [a,b,*]

[a] *Friedrich-Schiller-Universität Jena, Institut für Festkörperphysik, Helmholtzweg 3, D-07743 Jena, Germany*
[b] *Max-Planck-Institut für Astronomie, Königstuhl 17, D-69117 Heidelberg, Germany*

Received 25 July 2005; received in revised form 10 October 2005; accepted 13 October 2005
Available online 19 December 2005

Abstract

The electronic spectroscopy of polycyclic aromatic hydrocarbons (PAHs) is of particular interest for astrophysicists since these molecules are suggested as possible carriers of the diffuse interstellar bands. Here we report on our study of the $S_1 \leftarrow S_0$ transition of 2,3-benzofluorene (or benzo[b]fluorene) in the gas phase and in He droplets using cavity ring-down spectroscopy in a supersonic jet expansion and molecular beam depletion spectroscopy, respectively. The same techniques were also employed to identify the PAHs contained in the carbonaceous powder which was produced by CO_2 laser pyrolysis of a mixture of ethylene and benzene vapor. Phenanthrene and anthracene were unambiguously confirmed as components of the as-synthesized soot.

Keywords: Polycyclic aromatic hydrocarbons; PAHs; Diffuse interstellar bands; DIBs; Cavity ring-down spectroscopy; CRDS; Helium nanodroplets; Molecular beam depletion spectroscopy; MBDS

1. Introduction

Neutral and ionized polycyclic aromatic hydrocarbons (PAHs) have been postulated to be present in the interstellar medium [1] and to account for some of the so-called diffuse interstellar bands (DIBs) [2], still unassigned astrophysical absorption features observed in the spectra of reddened stars. Although discovered in the twenties of the last century, they still represent one of the mysteries in astronomy. Despite the importance of this class of molecules for astrophysics and nanophysics (PAHs can be regarded as nanoscale fragments of a sheet of graphite), the spectroscopic characterization of PAHs under well-defined conditions has remained a challenge. To improve this situation and to provide more laboratory data that can be compared with astronomical observations, we have initiated a research program to study the electronic spectroscopy of PAH molecules under astrophysically relevant conditions, i.e. at low temperature and so low density that the molecules do not interact. For this purpose, the molecules are studied in the expansion of a supersonic jet using the highly sensitive photoabsorption technique called cavity ring-down spectroscopy (CRDS). In this technique, the decay of the radiation from a pulsed tunable laser is measured at the exit of a high-quality resonator containing the molecules to be studied. The decay time can be directly converted to an absorption cross section. So far, with this technique, we have investigated the neutral PAHs anthracene [3] and pyrene [4] as well as the cations of naphthalene and anthracene [5]. Electronic CRDS studies on PAHs carried out by other researchers in supersonic jets include the cations of naphthalene [6,7,8], acenaphthene [7,8], and pyrene [8], as well as the neutrals of perylene [9] and benzo[ghi]perylene [10].

These true gas phase studies are complemented by absorption experiments of PAH molecules embedded in liquid helium droplets. In contrast to conventional matrix spectroscopy in argon or neon matrices, which suffers from the fact that the electronic absorption bands are significantly broadened and shifted with respect to the gas phase bands, the helium droplet provides a medium in which the interaction between the molecule and the rare gas atoms is minimized [11]. There is still a matrix effect, but the shifts are generally much smaller and the band widths much narrower. On the other hand, some advantages of matrix spectroscopy are kept, for example the possibility to collect the molecules for a longer time so that not so high vapor pressures are required as in gas phase

* Corresponding author. Address: Friedrich-Schiller-Universität Jena, Institut für Festkörperphysik, Helmholtzweg 3, D-07743 Jena, Germany. Tel.: +49 3641 947 354; Fax: +49 3641 947 308.
E-mail address: friedrich.huisken@uni-jena.de (F. Huisken).

0022-2860/$ - see front matter © 2005 Elsevier B.V. All rights reserved.
doi:10.1016/j.molstruc.2005.10.019

experiments. Moreover, the helium droplets provide a constant extremely low temperature of 380 mK for all degrees of freedom. The PAH spectral studies in He droplets are performed by molecular beam depletion spectroscopy (MBDS) or laser induced fluorescence (LIF) spectroscopy. Up to now, the PAH molecules that we have investigated in He droplets include anthracene [12,13], tetracene [12], and pyrene [4]. Using the same technique, Toennies and co-workers studied the PAHs tetracene and pentacene [11]. Very recently, emission spectra of tetracene, pentacene, and perylene in helium droplets were reported by Lehnig and Slenczka [14].

In this paper, we present our preliminary results on another PAH molecule, 2,3-benzofluorene or benzo[b]fluorene (Bzf, $C_{17}H_{12}$), that we have studied both in supersonic jet expansions and in helium droplets. The $S_1 \leftarrow S_0$ transition was investigated in the spectral range from 322 to 335 nm, which contains the origin band and vibrational bands with energies smaller than 1200 cm^{-1}. Neither gas phase nor helium droplet studies of Bzf in this spectral range were available up to now.

Besides commercially available PAHs, we have also investigated the carbonaceous powder that was synthesized by CO_2 laser pyrolysis of a 2:1 mixture of ethylene and benzene vapor. The resulting soot was expected to contain a large amount of PAHs [15] as could be verified by FTIR spectroscopy of the extract obtained by dissolving the soot in toluene and evaporating the solvent [16]. Moreover, UV spectra taken from the toluene extract dissolved in hexane suggested that the 3-ring PAHs phenanthrene and anthracene should be major components [16]. In order to confirm this finding, we have investigated the soot as well as the toluene extract using both spectroscopic techniques discussed before, i.e. cavity ring-down and helium droplet spectroscopy. The present investigation has been focused on the detection of the isomers phenanthrene and anthracene ($C_{14}H_{10}$) as components of the samples.

2. Experimental

2.1. Cavity ring-down laser absorption spectroscopy

The experimental setup has been described in detail elsewhere [3]. The PAH source consists of a pulsed 1-mm-diameter pinhole nozzle driven by a Series 9 valve supplied by Parker Hannifin Corporation (General Valve Division). The sample is contained in a reservoir located inside the valve and close to the nozzle, and can be heated up to 500 °C to provide a sufficiently high vapor pressure for the PAH under study. In almost all experiments, argon (Linde, purity 99.999%) is used as carrier gas.

The source is placed into a vacuum chamber onto which the cavity ring-down spectrometer is mounted. It is based on the original setup described by O'Keefe and Deacon [17]. The laser source consists of a pulsed tunable dye laser (Continuum TDL 60) pumped by the second harmonic ($\lambda = 532$ nm) of a Nd:YAG laser (Quantel YG-581-20) operated at a repetition rate of 20 Hz. The dye laser beam, frequency-doubled by a KDP crystal, is coupled into the CRDS cavity, which is formed by two plano-concave mirrors with a radius of curvature of 250 mm. The cavity length is 420 mm. In the present experiment, three different sets of mirrors were used. Their reflectances were 99.84% at 361 nm (Layertec GmbH), 99.76% at 330 nm (Layertec GmbH), and 99.5% at 283 nm (Laseroptik GmbH). The light transmitted by the rear mirror of the cavity was detected by a photomultiplier tube (Hamamatsu H6780-02) and its output signal digitized by a fast oscilloscope (Tektronix TDS 3052). Typically, at each wavelength, the signal was averaged over 64 laser shots, and the resulting decay function was transferred to a computer processing the signals and calculating the losses per pass. The wavelength calibration of the dye laser was carried out by using the absorption lines of metastable Ne observed by the optogalvanic effect in a Fe–Ne hollow cathode lamp (Hamamatsu L233-26NU). All wavelengths are given for vacuum. The laser linewidth is estimated to be 0.1 cm^{-1} in the visible [3].

2.2. Spectroscopy in helium droplets

The experiments devoted to the investigation of the absorption properties of PAHs in helium droplets were carried out in a molecular beam machine that has been described elsewhere [4,13]. Large helium clusters containing on the average $N \approx 8000$ helium atoms were produced by supersonic expansion of pure helium gas (Messer Griesheim GmbH, purity 99.9999%) at high pressure ($p = 20$ bar) through a 5-μm-diameter pinhole nozzle, cooled by liquid helium. The temperature of the nozzle was kept constant at $T = 13$ K and stabilized with an accuracy of better than 0.05 K. Since the helium clusters are liquid they are also referred to as droplets or nanodroplets. After preparation, the beam of helium nanodroplets was directed through a heatable cell (oven) containing approximately 1 cm^3 of the PAH sample. Upon collisions with the helium droplets, the sample molecules were embedded into the interior of the droplets and carried by them to the mass spectrometer detector. Before entering the detector chamber, the chromophore-containing helium cluster beam interacted with the pulsed radiation of a tunable dye laser.

In case of resonance, the laser radiation is absorbed by the PAH molecule in the helium droplet. Two processes are competing in the relaxation of the excitation energy: photoemission (fluorescence) and transfer of the electronic and/or rovibrational energy to the helium cluster. The transfer of the excitation energy to the helium cluster induces the evaporation of a few hundred to thousand helium atoms. This evaporation results in a broadening of the angular distribution of the cluster beam and in a reduction of the ionization cross section, both giving rise to a reduction of the molecular beam signal measured with the mass spectrometer detector on the mass of the PAH molecule. The latter technique, termed molecular beam depletion spectroscopy (MBDS), is exclusively used in the present study.

The laser system used for MBDS consists of a tunable dye laser (Lambda Physik SCANMATE 1) pumped by the second harmonic of a 10-Hz pulsed Nd:YAG laser (Continuum model NY81). The dye laser was operated with either DCM or

Rhodamine 6G, and its output was doubled in a KDP crystal. The laser linewidth was 0.24 cm^{-1} before doubling. The maximum pulse energy was around 500 μJ in the UV. The wavelength calibration was performed as in the CRDS experiment.

3. Results and discussion

3.1. 2,3-benzofluorene

The molecular structure of 2,3-benzofluorene (Bzf) is depicted in Fig. 1. It is characterized by 1+2 benzene rings with a five-fold ring in between giving rise to a bent structure with only one symmetry element (except of the identity), a plane of symmetry. Neither gas phase nor helium droplet spectra were available for this molecule. However, we could resort to argon matrix isolation studies [18,19] which were helpful to locate the origin of the $S_1 \leftarrow S_0$ transition in the gas phase.

Fig. 1 shows the $S_1\,(^1A') \leftarrow S_0\,(^1A')$ origin band measured by CRDS in the expansion of a supersonic jet, 4.6 mm downstream from the nozzle exit (solid line). The valve was operated at a temperature of 170 °C, and Ar was used as carrier gas (p_{Ar} = 2.5 bar). The structure in the band profile corresponds to P and R rotational branches. The S_0 and S_1 states of Bzf transform according to the A' irreducible representation of the C_s point group. Therefore the vibrationless transition between these two electronic states has to show a hybrid *A*- and *B*-type rotational profile. Rotational constants were determined for the equilibrium geometry of both electronic states while carrying out ab initio calculations with the GaussianW03 package [20]. The configurations of Bzf in the S_0 and S_1 states were tightly optimized in the frozen core approximation, at the RHF/6-31+G(d,p) and RCIS/6-31+G(d,p) levels, respectively. The calculated rotational constants are $A = 0.0528082\ cm^{-1}$, $B = 0.0089092\ cm^{-1}$, and $C = 0.0076339\ cm^{-1}$ for the ground state. They are $A' = 0.0516080\ cm^{-1}$, $B' = 0.0089539\ cm^{-1}$, and $C' = 0.00764095\ cm^{-1}$ for the excited state. The RCIS calculation also yielded the projections of the transition dipole moment on the principal axis of inertia, indicating that the vibrationless transition is 81% *A*-type. Rotational contour simulations of the $S_1\,(0) \leftarrow S_0\,(0)$ transition were carried out with the SpecView program of Stakhursky and Miller [21]. The best simulation is obtained for a rotational temperature of 12 K and is shown in Fig. 1 by the dashed line. The band center of the $S_1\,(0) \leftarrow S_0(0)$ transition, as determined while optimizing the simulated profile, is 29 894.3 cm^{-1}.

The origin band measured in He droplets is shown in Fig. 2 together with the gas phase spectrum just discussed. It is noted that the He droplet spectrum is shifted by 5.1 cm^{-1} to higher wave numbers. Although broadened by the phonon wing, the band observed in helium droplets comes close to the gas phase data (FWHM is 1.6 cm^{-1} for the gas phase spectrum and 12 cm^{-1} for the phonon wing-broadened helium droplet band). Compared to other PAHs that we have studied in helium droplets (e.g. anthracene and tetracene [13]), in the case of Bzf, the splitting of the zero phonon line shows multiple peaks separated by 1.5–2.3 cm^{-1}. This splitting can be explained by a coupling with the vibrational modes of the first closed shell of He atoms surrounding the Bzf molecule.

Fig. 3 presents the Bzf spectra that we have recorded in the wave number range from 29 800 to 31 000 cm^{-1}. The gas phase spectrum measured for a nozzle temperature of 200 °C is displayed in the bottom panel. The bands at higher energies than the origin band at 29 894.3 cm^{-1} belong to vibronic transitions from the $v = 0$ level of the ground state to excited vibrational levels in the S_1 state.

High-resolution matrix spectra of Bzf were first reported by Nakhimovsky et al. [22] using a *n*-hexane matrix at 5 K. For each band, the spectra showed a multiplet structure caused by the various orientations of the embedded molecule. The newer high-resolution spectra of Bzf obtained by Geigle and

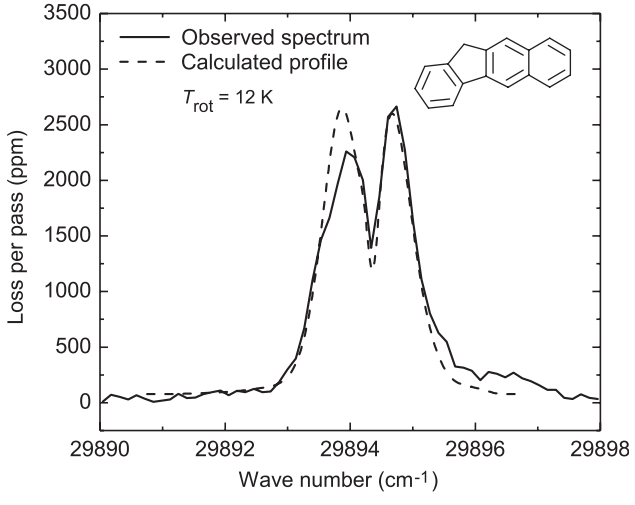

Fig. 1. The $S_1\,(^1A') \leftarrow S_0(^1A')$ origin band of 2,3-benzofluorene in the gas phase as obtained by CRDS (solid line). The dashed line corresponds to a numerical simulation of the rotational contour. A rotational temperature of 12 K is estimated at 4.6 mm distance from the nozzle exit.

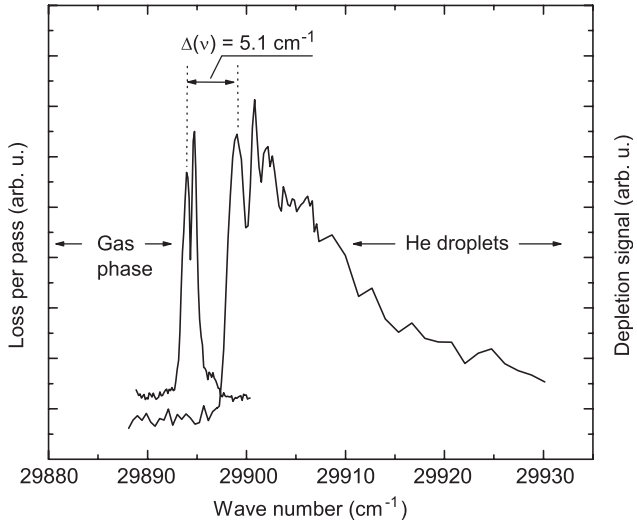

Fig. 2. The origin band of the $S_1 \leftarrow S_0$ transition of 2,3-benzofluorene in He droplets obtained by MBDS and shown in comparison with the gas phase spectrum.

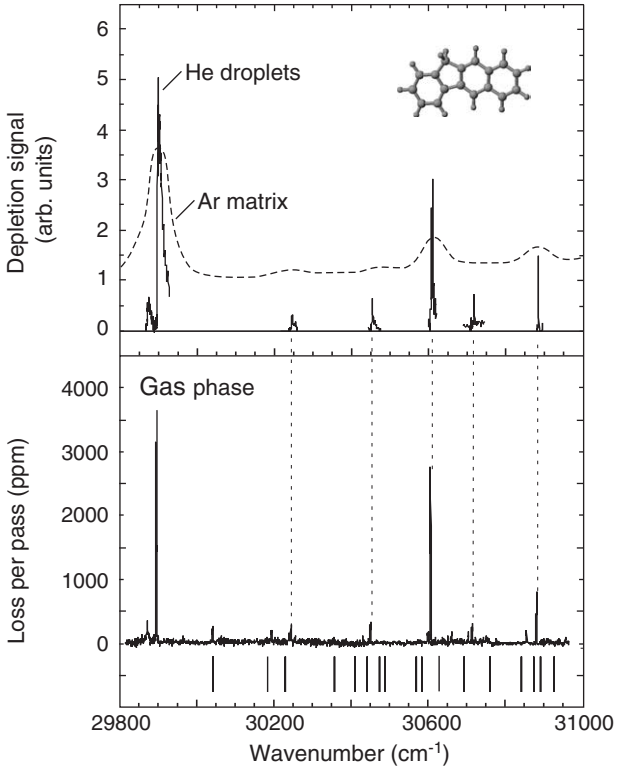

Fig. 3. $S_1 \leftarrow S_0$ absorption spectra of 2,3-benzofluorene measured in the gas phase (supersonic jet) by CRDS (bottom panel) and in helium droplets by MBDS (upper panel). The conventional Ar matrix spectrum plotted in the upper panel was adopted from Banisaukas et al. [19]. The vertical lines given below the gas phase spectrum mark the frequency positions obtained from ab initio calculations.

Hohlneicher [18] at 14 K in an Ar matrix were free of multiplet structures as they used site-selective laser excitation/fluorescence spectroscopy. As far as the vibronic band intensities and their positions relative to the origin band are concerned, their excitation spectrum resembles very much our gas phase spectrum. However, the vibronic bands are approximately three times broader and the entire spectrum is shifted by approximately 240 cm^{-1} to the red. Although, compared to the *n*-hexane matrix, the red shift was reduced by a factor of more than 2, it is still quite pronounced. The most recent Ar matrix isolation study was carried out by Banisaukas et al. [19] using a conventional UV spectrometer. Concentrating on the spectral range discussed here, we adopted their spectrum and included it in the upper panel of Fig. 3 (after it was shifted by 246 cm^{-1} to the blue). It is clearly seen that all spectral features of the Ar matrix spectrum find their counterparts in the gas phase spectrum. However, with widths around 70 cm^{-1}, the bands are much broader than observed in the gas phase ($\sim$1.6 cm^{-1}) and also in the earlier site-selective matrix experiment ($\sim$5 cm^{-1}) [18]. With our study, the red shift produced by the argon matrix can be given to be 233.3 cm^{-1} [18] or 247.1 cm^{-1} [19], depending on what matrix data is taken for comparison. Table 1 compares the band parameters observed in the supersonic jet with those measured in the various matrix materials discussed.

Table 1
Parameters of the origin band of the $S_1(^1A') \leftarrow S_0$ ($^1A'$) transition of 2,3-benzofluorene observed in a supersonic jet and various matrix materials

Condition	Band position [cm^{-1}]	Shift [cm^{-1}]	Width (FWHM) [cm^{-1}]
Supersonic jet[a]	29 894.3	0	1.6
He droplets[a]	29 899.4	+5.1	12
Ar matrix with site selection[b]	29 661	−233	5
Conventional Ar matrix[c]	29 647	−247	71
n-hexane matrix[d]	29 304	−590	~170

[a] This work.
[b] Geigle and Hohlneicher [18].
[c] Banisaukas et al. [19].
[d] Nakhimovsky et al. [22].

Using Gaussian ab initio calculations carried out at the same level as mentioned above, we have determined the energies of the fundamental vibrations in the electronically excited S_1 state. After scaling the values with the factor 0.9, the corresponding transition frequencies from the S_0 vibrational ground state were derived. They are given in Fig. 3 by the vertical lines plotted below the gas phase spectrum. Only the totally symmetric modes were taken into account since transitions to non-totally symmetric levels are not allowed within the Franck-Condon approximation. Using the MolFC program developed by Borrelli [23], we made an attempt to determine the intensities of the vibronic bands, but the agreement between experiment and calculation was rather poor. Indeed, as has been pointed out by Geigle and Hohlneicher [18], due to the vibronic coupling between S_1 and higher electronic states, Herzberg-Teller interferences must be taken into account to correctly predict the band intensities. Advanced calculations are in progress to properly assign the vibronic transitions observed in the present study [24].

Some of the bands including the origin band have also been measured in helium droplets employing the molecular beam depletion technique with the mass spectrometer tuned to the mass of Bzf (m=216 amu). The results are plotted in the upper frame of Fig. 3. It is important to note that the bands measured in helium droplets have not been shifted in frequency. In contrast to other PAH molecules studied before, it appears that, for Bzf, the frequency shifts induced by the helium matrix are very small (blue shifts between 3.2 and 6.5 cm^{-1}).

Discussing frequency shifts for different molecules as a function of the matrix material is not an easy task since the total shift is composed of two contributions, an attractive and a repulsive term. Obviously an increase of the attraction experienced by the molecule and the surrounding matrix during the transition results in a red shift. On the other hand, a stronger repulsion between the molecule and the matrix after the excitation will produce a blue shift. It can be predicted that the change in attraction is proportional to the polarizability. In case of electronic transitions, the change of the repulsive term is not predictable. It depends on the electronic structure and on what electrons are involved in the transition. For an argon

matrix, the attraction is in almost all cases the dominant term yielding a pronounced red shift. In contrast, in helium droplets, the attractive contribution is much smaller so that the repulsive term may prevail, finally resulting in a small blue shift. Apparently, this situation is encountered in the case of 2,3-benzofluorene.

Particularly interesting are the features observed on the red side of the origin band in both spectra (-22 and $-26.5\ cm^{-1}$ in the gas phase and helium droplet spectra, respectively). In our gas phase studies, we observed that this band did not change in intensity when the valve temperature was varied between 175 and 240 °C while all other bands strongly increased in intensity when the temperature was raised. This behavior suggested that the band on the red side should be assigned to the Bzf·Ar van der Waals complex. Indeed, the proof for this interpretation was given when we used neon instead of argon as carrier gas, for the peak was absent. This explanation cannot be given for the small band observed in helium droplets at the equivalent position. Clearly, the coincidence must be considered as accidental. Further investigations are necessary to reveal the nature of this peak in helium droplets.

3.2. Carbonaceous powder

The general idea of the following experiment results from the fact that one has already measured the spectra of several commercially available PAH molecules, but up to now no correspondence with any DIB was found. Perhaps some DIBs are due to not so common PAHs and possibly such molecules can be synthesized in free chemistry processes. It is known that PAH-containing soot can be produced in flames and in laser pyrolysis experiments using hydrocarbons as precursors. In the present experiment, we have studied the carbonaceous soot obtained by laser pyrolysis of a 2:1 mixture of ethylene and benzene vapors using a continuous-wave CO_2 laser with a power of 600 W [15]. The conditions were adjusted so as to obtain high concentrations of PAHs. Indeed, gas chromatography mass spectra of the samples revealed high concentrations of PAHs and UV spectra taken from the toluene extract in hexane suggested that the 3-ring PAHs phenanthrene and anthracene should be a major component [16].

Employing the CRDS and MBDS techniques described in the experimental part and applied to 2,3-benzofluorene, we have investigated both the carbonaceous powder as it was synthesized in the laser pyrolysis process as well as the extract which was obtained by dissolving the carbonaceous powder in toluene, filtering the solution, and finally evaporating the solvent.

Our first studies were devoted to the investigation of the samples by incorporating the volatile molecules into helium droplets. In Fig. 4, we present the mass spectrum that we could measure when the extract was evaporated close to the helium droplet beam at a temperature of 140 °C. It reveals the mass distribution of the molecules which were actually carried by the helium droplets to the mass spectrometer detector. Besides the rather intense mass peak at 178 amu, probably caused by

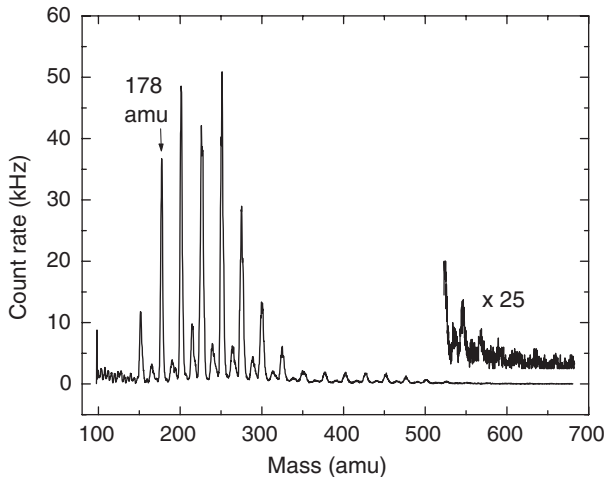

Fig. 4. Mass spectrum recorded for laser pyrolysis soot. The sample was evaporated at 140 °C and deposited into helium droplets.

anthracene and phenanthrene (both molecules have the same mass), other mass peaks corresponding to aromatic hydrocarbons with masses up to ~650 amu are detected. Interestingly, two alternations with strong and weak peak intensities are observed. The average distance between two peaks in each alternation corresponds to 25 amu, suggesting that, during the growth of the PAHs, the addition of two carbon and one hydrogen atom was favored (on the average). This successive growth mechanism complies with the hydrogen-abstraction-C_2H_2-addition (HACA) route widely used in modelling studies carried out to explain the PAH formation in combustion environments [25].

To identify the species giving rise to the signal on mass $m=178$ amu, we have measured depletion spectra with the mass spectrometer fixed to this mass and the laser beam tuned around the absorption band of phenanthrene. For a proper comparison and prior to this experiment, we have determined the absorption profile of phenanthrene (Aldrich, purity 98%) as a pure substance employing the same conditions. Up to now, no other studies of phenanthrene in He droplets were reported in the literature. In Fig. 5, the $S_2\ (^1B_2) \leftarrow S_0\ (^1A_1)$ origin band of phenanthrene as measured in helium droplets is plotted by the solid curve. The dashed and dotted curves represent the spectra as obtained from the soot and extract, respectively. The close resemblance of the absorption bands clearly reveals that phenanthrene is a constituent of all samples. The smaller depletion signals measured for the soot and extract (19% depletion compared to 45% for the pure substance) indicate that only 42% of the total count rate at mass $m=178$ amu originates from phenanthrene. The remaining 58% must be due to other molecules with the same mass (for example anthracene) or fragments of larger PAHs to this mass. Compared to the respective gas phase transition to be reported below, the helium droplet spectra reveal a matrix shift of $-62\ cm^{-1}$ and exhibit substantial broadening. This is however difficult to quantify since the helium droplet spectra were measured at higher laser energy so that power broadening is effective.

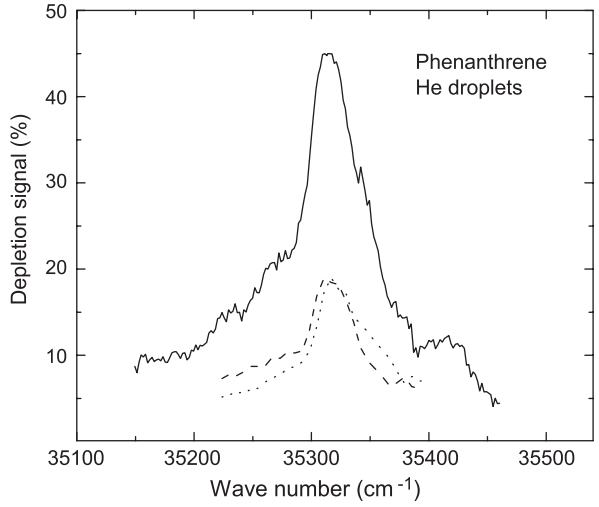

Fig. 5. The S_2 ($^1B_2$)←S_0 ($^1A_1$) origin band of phenanthrene measured by MBDS in helium droplets. The solid curve refers to the pure substance of phenanthrene while the dashed and dotted lines correspond to phenanthrene spectra obtained from laser pyrolysis soot and the extract thereof, respectively. The soot and extract samples were heated to 100 °C while the pure substance was kept at −7 °C.

The presence of phenanthrene in the soot and extract samples was also confirmed by gas phase studies carried out with our CRDS setup. As for the He droplet studies, the $S_2 \leftarrow S_0$ origin band of phenanthrene was used for the investigation in the gas phase. The position of this band was previously determined in a LIF study of phenanthrene in a supersonic jet (35 375 cm^{-1}) [26] and we found it at 35 378.2 cm^{-1}. Fig. 6 shows the $S_2 \leftarrow S_0$ origin band of phenanthrene as recorded for the pure chemical substance (solid line) as well as for the soot (dashed curve) and extract (dotted curve) samples. The smaller amplitudes of the soot and extract peaks in the CRDS spectra (compared to the intensity of the pure substance) merely reflect the fact that the phenanthrene densities were lower when the

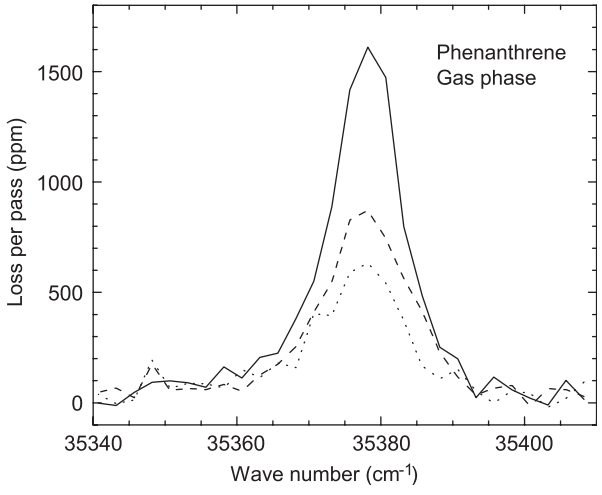

Fig. 6. Phenanthrene absorption spectra measured by CRDS in supersonic jets. The meaning of the solid, dashed, and dotted curves is the same as in Fig. 5. The soot and extract samples were heated to 130 °C while the pure substance was kept at 100 °C.

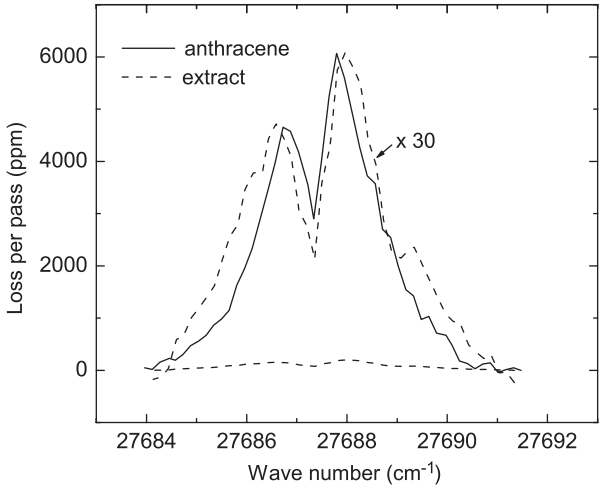

Fig. 7. The origin band of the S_1 ($^1B_{2u}$)←S_0 (^1A_g) transition of anthracene measured by CRDS in supersonic jets for the pure chemical substance (solid line) and the extract of the soot obtained by laser pyrolysis (dashed lines).

soot/extract samples were evaporated at the same temperature of 130 °C.

The next experiment was devoted to the identification of anthracene in our laser pyrolysis samples. Due to the same mass of anthracene and phenanthrene and the large abundance of phenanthrene, we were not able to observe a depletion signal on $m = 178$ amu in the helium droplet experiment when the laser was tuned to the absorption frequency of anthracene [13]. This failure is putting an upper limit of 5% for the concentration of this species in our samples. In contrast, our CRDS gas phase investigation unambiguously confirms the presence of anthracene in the extract sample. Fig. 7 shows the S_1 ($^1B_{2u}$)←S_0 (^1A_g) origin band of anthracene measured by CRDS for the pure chemical substance (Aldrich, purity 97%) (solid line) and the extract (dashed lines). The signal from the extract is 30 times lower than that obtained from chemically pure anthracene at the same valve temperature of 180 °C. Based on the approximation that the same vapor pressure is achieved for both samples, we can estimate that the concentration of anthracene in the extract is approximately 3.3%, which is consistent with the 5% upper limit determined in the MBDS experiment.

4. Conclusions

In this paper, we have presented new results on the absorption spectroscopy of 2,3-benzofluorene for the transition from the S_0 electronic ground state to the first singlet excited state, S_1. The studies were conducted in the gas phase using cavity ring-down spectroscopy in combination with supersonic jets and in helium droplets employing molecular beam depletion spectroscopy. The position of the S_1 (0)←S_0 (0) transition was located at 29 894.3 cm^{-1} (334.5 nm). While the same transition in helium droplets is only shifted by 5.1 cm^{-1} to the blue, the matrix shift for argon was determined to be around 240 cm^{-1} to the red. Various yet unassigned vibrational bands were measured on the blue side of the origin

band. For all of them, the blue shift caused by the helium droplets was smaller than 6.5 cm^{-1}. It is concluded that helium droplet spectra are much better suited for comparison with astronomical data than neon or even argon matrix data, if gas phase spectra are not available or too difficult to obtain. Since the absorption features of 2,3-benzofluorene are in the UV this molecule cannot be responsible for any of the major diffuse interstellar bands.

In a completely different approach, we have investigated the carbonaceous soot produced by laser pyrolysis of a mixture of hydrocarbons and benzene vapor. Mass spectra revealed that the soot contained various PAHs with masses up to 650 amu which are difficult to identify. The presence of phenanthrene was confirmed by measuring its absorption spectrum in the gas phase and in helium droplets. Because of the low concentration achieved in the gas phase, the stronger $S_2 \leftarrow S_0$ transition was chosen to monitor the molecule (instead of $S_1 \leftarrow S_0$). Anthracene was analyzed in the samples employing cavity ring-down spectroscopy and probing the $S_1 \leftarrow S_0$ transition.

It was found that the laser pyrolysis soot provides samples which could be very interesting for laboratory astrophysics applications. While the present study focused only on the three-ring PAHs phenanthrene and anthracene, further investigations are in progress to identify the larger PAHs in the soot, which are expected to have their absorption bands in the visible, i.e. in the same region where the DIBs are observed, and to study their spectroscopy.

Acknowledgements

This work was supported by a cooperation between the Max-Planck-Institut für Astronomie and the Friedrich-Schiller-Universität Jena as well as by the Deutsche Forschungsgemeinschaft in the frame of the Forschergruppe Laborastrophysik. The authors are grateful to I. Voicu for the synthesis of the PAH-containing powder by laser pyrolysis, to C. Jaeger for analyzing this powder, and to M. Vala for providing computational results for the vibrations of 2,3-benzofluorene in its electronic ground state.

References

[1] F. Salama, G.A. Galazutdinov, J. KreŁowski, L.J. Allamandola, F.A. Musaev, Astrophys. J. 526 (1999) 265.
[2] P. Jenniskens, F.-X. Désert, Astron. Astrophys. Suppl. Ser. 106 (1994) 39.
[3] A. Staicu, G. Rouillé, O. Sukhorukov, Th. Henning, F. Huisken, Mol. Phys. 102 (2004) 1777.
[4] G. Rouillé, S. Krasnokutski, F. Huisken, Th. Henning, O. Sukhorukov, A. Staicu, J. Chem. Phys. 120 (2004) 6028.
[5] O. Sukhorukov, A. Staicu, E. Diegel, G. Rouillé, Th. Henning, F. Huisken, Chem. Phys. Lett. 386 (2004) 259.
[6] D. Romanini, L. Biennier, F. Salama, A. Kachanov, L.J. Allamandola, F. Stoeckel, Chem. Phys. Lett. 303 (1999) 165.
[7] L. Biennier, F. Salama, L.J. Allamandola, J.J. Scherer, J. Chem. Phys. 118 (2003) 7863.
[8] L. Biennier, F. Salama, M. Gupta, A. O'Keefe, Chem. Phys. Lett. 387 (2004) 287.
[9] X. Tan, F. Salama, J. Chem. Phys. 122 (2005) 084318.
[10] X. Tan, F. Salama, J. Chem. Phys. 123 (2005) 014312.
[11] J.P. Toennies, A.F. Vilesov, Angew. Chem. Int. Ed. 43 (2004) 2622.
[12] F. Huisken, S. Krasnokutski, in: E.P. Muntz, A. Ketsdever (Eds.), Proceedings of the 23rd International Symposium on Rarified Gas Dynamics, Whiley, New York, 2002, p. 678.
[13] S. Krasnokutski, G. Rouillé, F. Huisken, Chem. Phys. Lett. 406 (2005) 386.
[14] R. Lehnig, A. Slenczka, J. Chem. Phys. 122 (2005) 244317.
[15] I. Voicu, private communication, 2005.
[16] C. Jaeger, I. Voicu, A. Staicu, S. Krasnokutski, F. Huisken, in preparation.
[17] A. O'Keefe, D.A.G. Deacon, Rev. Sci. Instrum. 59 (1988) 2544.
[18] K.P. Geigle, G. Hohlneicher, J. Mol. Struct. 480-481 (1999) 247.
[19] J. Banisaukas, J. Szczepanski, M. Vala, S. Hirata, J. Phys. Chem. A 108 (2004) 3713.
[20] M.J. Frisch, G.W. Trucks, H.B. Schlegel, et al., GAUSSIAN 03W, Revision C. 02, Gaussian, Inc., Pittsburgh, PA, 2003.
[21] V. Stakhursky, T.A. Miller, SpecView: Simulation and fitting of rotational structure of electronic and vibronic bands, 56th Molecular Spectroscopy Symposium; http://molspect.mps.ohio-state.edu/goes/spec-view.html
[22] L.A. Nakhimovsky, M. Lamotte, J. Joussot-Dubien, Handbook of Low Temperature Electronic Spectra of Polycyclic Aromatic Hydrocarbons, Elsevier, Amsterdam, 1989.
[23] R. Borrelli, A. Peluso, J. Chem. Phys. 119 (2003) 8437http://pcdual.chem.unisa.it/; A. Peluso, F. Santoro, G. Del, Int. J. Quant. Chem. 63 (1997) 233.
[24] A. Staicu, S. Krasnokutski, G. Rouillé, F. Huisken, Th. Henning, R. Scholz, S. Rastogi, in preparation.
[25] H. Wang, M. Frenklach, Combust. Flame 110 (1997) 173.
[26] N. Ohta, H. Baba, Mol. Phys. 59 (1986) 921.